Food Control 140 (2022) 109128

Contents lists available at ScienceDirect

Food Control

journal homepage: www.elsevier.com/locate/foodcont

Development of active films utilizing antioxidant compounds obtained from tomato and lemon by-products for use in food packaging

Sandra Mariño-Cortegoso [a], Mariamelia Stanzione [b], Mariana A. Andrade [c,d,e], Cristina Restuccia [f], Ana Rodríguez-Bernaldo de Quirós [a], Giovanna G. Buonocore [b], Cássia H. Barbosa [c,g], Fernanda Vilarinho [c], Ana Sanches Silva [h,i], Fernando Ramos [d,e], Khaoula Khwaldia [j], Raquel Sendón [a], Letricia Barbosa-Pereira [a,*]

[a] Analytical Chemistry, Nutrition and Food Science Department, Pharmacy Faculty, University of Santiago de Compostela, Santiago de Compostela, Spain
[b] Institute for Polymers, Composites and Biomaterials (IPCB-CNR), Portici, NA, Italy
[c] Department of Food and Nutrition, National Institute of Health Dr. Ricardo Jorge, Av. Padre Cruz, 1649-016, Lisbon, Portugal
[d] University of Coimbra, Faculty of Pharmacy, Coimbra, Azinhaga de Santa Comba, 3000-548, Coimbra, Portugal
[e] REQUIMTE/LAQV, University of Porto, R. D. Manuel II, Apartado, 55142, Oporto, Portugal
[f] Department of Agriculture, Food and Environment (Di3A), University of Catania, via Santa Sofia 100, Catania, 95123, Italy
[g] Department of Sciences and Technology of Biomass, NOVA School of Science and Technology, Caparica, Portugal
[h] National Institute for Agricultural and Veterinary Research (INIAV), I.P., Rua dos Lagidos, Lugar da Madalena, 4485-655, Vairão, Vila do Conde, Portugal
[i] Center for Study in Animal Science (CECA), ICETA, University of Oporto, 4051-501, Oporto, Portugal
[j] Laboratoire des Substances Naturelles, Institut National de Recherche et d'Analyse Physico-Chimique (INRAP), Pôle Technologique de Sidi Thabet, Tunisia

ARTICLE INFO

Keywords:
Food active packaging
Food by-products
Polyphenols
Antioxidant capacity
HPLC-DAD-ESI-MS/MS
LDPE
PLA
GP

ABSTRACT

This study focused on the recovery of antioxidant compounds from lemon and tomato by-products for use as natural additives in the development of active food packaging formulated using three different polymeric matrices that included low-density polyethylene (LDPE), polylactic acid (PLA), and G-polymer (GP). The films were characterized according to chemical-physical, thermal analyses, and their barrier and mechanical properties. Migration assays were performed to evaluate the release of active compounds from polymeric matrices, which were quantified in the food simulant by high-performance liquid chromatography with a diode array detector and then confirmed via liquid chromatography coupled to mass spectrometry. The antioxidant capacities of the films were determined to evaluate their applicability for use as antioxidant-active packaging. The incorporation of extracts into polymers resulted in different structural changes and enhanced properties according to the nature of the polymeric matrix based on the interactions of the –OH groups of polyphenols and the chemical groups of the polymers. The lemon (LE) and tomato (TE) extracts lead to a substantial improvement in water barrier properties of PLA and GP-based films. The active PLA and GP films released high amounts of polyphenolic compounds (up to 65% for GP containing LE); mainly hesperidin and eriocitrin for LE films, and chrologenic acid for TE films. PLA loaded with lemon extract at 4% was selected as the most suitable for use as antioxidant packaging to extend the shelf-life of foods with high fat content.

1. Introduction

The food industry provides a diverse array of offerings with many natural products and their derivatives; however it is also responsible for producing a large amount and variety of by-products (Khedkar & Singh, 2018) that reached 88 million tons in 2012 at an equivalent cost of 143 billion euros as estimated by the EU (Stenmarck et al., 2016).

Mediterranean countries are large producers of citrus fruits and tomatoes, particularly in Spain and Italy. The annual production of citrus fruits and tomatoes from these nations was approximately 20 million tons in 2020/2021 (European Commission. Eurostat, 2021; European Commission. Eurostat, 2022). Other vegetables and fruit by-products have long been known to possess high antioxidant capacities and antimicrobial properties (Andrade et al., 2020; Barbosa et al., 2021;

* Corresponding author.
E-mail address: letricia.barbosa.pereira@usc.es (L. Barbosa-Pereira).

https://doi.org/10.1016/j.foodcont.2022.109128
Received 23 November 2021; Received in revised form 6 May 2022; Accepted 22 May 2022
Available online 25 May 2022

Faustino et al., 2019; Gowe, 2015), and they are a source of active compounds that are associated with human health benefits (Barbosa et al., 2021; Martí et al., 2017; Tamasi et al., 2019; Vallverdú-Queralt et al., 2011; Ćetković et al., 2012).

The antioxidant properties of fruit by-products promote their use as food additives that can extend food shelf-life. Moreover, consumers prefer natural antioxidants instead of synthetic food additives. This is based on the knowledge that natural additives are healthier than synthetic additives and on consumer awareness of the health benefits of a diet consisting of natural and fresh foods (Carocho et al., 2014). For these purposes, a number of natural extracts have been used as food additives in food packaging, thus generating the well-known active food packaging (Sanches-Silva et al., 2014; Susmitha et al., 2021; Vilarinho et al., 2021; Zeng et al., 2021). This type of packaging improves food quality by preventing spoilage and extending the food shelf-life (Abreu et al., 2012).

Among the vast number of fruit by-products, peels are one of the most common. Mango, orange, and pomegranate peels are frequently used in the production of active packaging possessing antioxidant properties (Adilah et al., 2018; Hanani et al., 2019; Jridi et al., 2019). In addition to conventional polymers, extracts of fruit by-products, such as gelatin or pectin are included in polymeric biodegradable matrices in a concept termed circular economy (Kurek et al., 2021; Rangaraj et al., 2021, 2022; Ribeiro et al., 2021). However, the physical properties of these edible films may be improved to allow for the same use and utility as conventional polymers.

Regarding traditional polymeric matrices used in food contact materials, LDPE is the most extended polymer for use in food packaging applications due to its low cost and desirable chemical and mechanical properties (Kormin et al., 2017). Studies often include its use as active packaging when incorporating active compounds from different sources, such as rosemary extract, natural extract from brewery wastes, grapes, turmeric, coffee, and orange wastes (Barbosa-Pereira et al., 2014; Giannakas et al., 2019; Iyer et al., 2016). In contrast, polylactic acid (PLA) is a biodegradable polymer that allows high release rates of active compounds (Jamshidian et al., 2013) using extracts from citrus peel or almond shell by-products or other sources (Fiorentini et al., 2022; Valdés et al., 2021). Another biodegradable polymer is the new highly amorphous vinyl alcohol, that has been commercialized with the trade name GP. This polymer exhibits improved properties compared to those of polyvinyl alcohol (PVOH), which is one of the most used water-soluble polymers (Russo et al., 2015). To the best of our knowledge, no data are available regarding the application of GP as an active film for food applications; however, its eco-friendly characteristics might be of interest for this purpose.

This study was focused on the development of active food packaging films based on the recovery of antioxidant compounds from lemon and tomato by-products used as natural additives. The natural extracts were incorporated into three different polymeric matrices (LDPE, PLA, and GP) to select the most suitable film possessing antioxidant properties. The physical and chemical characterization of the films, the determination of the phenolic compounds released, and the antioxidant capacity of the active films were assessed to evaluate their application as antioxidant-active packaging to extend the shelf-life of foods.

2. Materials & methods

2.1. Polymers & chemicals

High amorphous polyvinyl alcohol [G-Polymer, GP, grade OKS-8049 with viscosity 4.6 mPa s (4% aq at 20 °C)] was purchased from the Nippon Synthetic Chemical Industry Co., Ltd. (Japan). Low-density polyethylene (LDPE, Riblene FL30, with Melt Flow Rate 2.2 g/10 min at 190 °C/2.16 kg, density 0.923 g/cm^3, fusion point 110 °C) was purchased from Polimeri Europa (Italy). The poly (L-lactide) polymer (Ingeo™ Biopolymer 4032D, with specific gravity 1.24, MFR 7 g/10 min at 210 °C/2.16 kg, density 1.08 g/cm^3 at 230 °C, melting point 155–170 °C) was supplied by NatureWorks™ (Minnetonka, MN, USA). Prior to further processing, the PLA pellets were dried at 90 °C for at least 12 h under a vacuum due to their tendency to hydrolyze. Methanol LC-MS grade, methanol and ethanol, (both HPLC grade), were supplied by Merck (Darmstadt, Germany). Acetic acid was obtained from Sigma-Aldrich (Germany). Ultrapure water (Type I) was obtained using an automatic system of purification system (Wasserlab, Navarra, Spain).

Reference standards for individual phenolic compounds were provided by different providers. Catechin, epicatechin, rutin, naringenin, quercitrin, caffeic acid, *p*-coumaric acid, eriocitrin, and protocatechuic acid were purchased from Sigma-Aldrich (St Louis, MO, USA), gallic acid and chlorogenic acid were supplied by Fluka Chemie AG (Bus, Switzerland), *p*-hydroxybenzoic acid was provided by Alfa Aesar (Karlsruhe, Germany), and hesperidin was provided by USP (Twinbrook Pkwy, Rockville, MD, USA). All standards possessed purities ≥95%, with the exception of quercitrin at a purity of 78%.

2.2. Tomato & lemon by-products extracts

Tomato pomace (a mixture of peels, seeds, and small amounts of residual flesh) was industrially obtained through small-sized tomato processing (cherry and date tomatoes) and stored at −20 °C until extraction. Frozen pomace samples were ground using a home grinder (La Moulinette, Moulinex, 2002). An aliquot of approximately 150 g was mixed with 400 mL of three different solvents that included distilled water (W); distilled water: ethanol (75:25, WE); and distilled water: ethanol: formic acid (70:29:1, WEA). The extraction was performed overnight at 4 °C in the dark. After extraction, the samples were filtered using a Grade 1 Whatman® qualitative filter paper (Merck KgaA, Darmstadt, Germany) under vacuum. The ethanol from the WE and WEA extractions was evaporated using a rotavapor. The aqueous solutions that resulted from the three different extracts were frozen at −20 °C and then lyophilized. The extracts yielded were evaluated for total phenolic compounds (see 2.9.1) and radical scavenging activity (see 2.9.3). The tomato by-product extract with the highest antioxidant capacity was used for films preparation.

The lemon by-product was kindly supplied by the Portuguese juice company, Frubaça-Cooperativa de Hortofruticultores. The active extract was obtained via solid-liquid extraction using absolute ethanol, as described by Barbosa et al. (2021). Briefly, 50 mL of absolute ethanol was added to 5 g of sample. The mixture was agitated on a compact shaker (Edmund Bühler GmbH model KS-15, Hechingen, Germany) at 450 rpm for 30 min at room temperature (23 ± 1 °C) while being protected from light. The mixture was then centrifuged (Heraeus Multifuge X3 FR, Thermo Scientific, Langenbold, Germany) at 6000 rpm at 10 °C for 10 min. Next, the supernatant was removed into a pear-shaped amber flask, and the ethanol was completely evaporated on a rotary evaporator (Büchi model R-210 Labortechnik, Switzerland) at 35 °C. The extract was removed with the aid of a spatula, stored at −20 °C, and protected from the light until further use. The FTIR spectra of the obtained extracts are presented in Fig. S3.

2.3. Preparation of films formulations

The processing variables used to produce films containing active substances were identified and later optimized. The LDPE, PLA, and GP films containing the active substances (lemon or WE-tomato by-product extracts coded as LE and TE, respectively) were prepared by direct melt processing in a two-step procedure that included melt mixing and hot compression. In detail, both extracts at a concentration of 4% weight content of polymer matrices (w/w), were mixed with PLA, LDPE, and GP in an internal mixer (Rheomix® 600 Haake, Germany) with a volumetric capacity of 50 cm^3 at 170 °C, 180 °C and 200 °C, respectively, and at 50 rpm for 5 min. This percentage of extract was selected as the optimal amount based on film processability and preliminary antioxidant tests.

Composite films were prepared by hot pressing the obtained matter using a Collin P300P press at the previous three different temperatures (P = 50 bar for 3 min). Six different polymer-based active composites, coded as PLA_4LE, PLA_4 TE, LDPE_4LE, LDPE_4 TE, GP_4LE, and GP_4 TE that were obtained with thickness of approximately 100–150 μm. For comparison purposes, neat PLA, LDPE, and GP films were manufactured under the same specific processing conditions.

2.4. Characterization of active films

2.4.1. Fourier transform infrared spectroscopy (FTIR) of composite films

FTIR spectra were recorded at room temperature, using an FTIR spectrometer (model Frontier Dual Ranger, PerkinElmer, USA) in attenuated total reflectance mode from to 650–4000 cm^{-1}. Spectra were obtained at a resolution of 4 cm^{-1}, and the reported results are the average of 64 scans.

2.4.2. Thermal analysis (thermogravimetric analyses (TGA) and differential scanning calorimetry (DSC) of active films

Thermogravimetric analyses (TGA) were performed by using a TGAQ500 instrument, (TA Instruments). The samples were heated in a nitrogen flow up to 800 °C at a heating rate of 10 °C/min.

DSC tests were performed in a heat-cool-heat mode. The sample (10–15 mg) was placed in a DSC pan and heated from −80 °C to 250 °C at 10 °C/min. The acquired data were analyzed using the Universal Analysis software to compute the necessary parameters.

2.4.3. Contact angle measurements of composite films

Contact angle measurements were performed using a DataPhysics OCA 20 apparatus. Distilled water was dropped onto at least 10 different sites on each sample, and the static contact angle was reported as the average value of each individual measurement (Stanzione et al., 2017, p. pp88).

2.4.4. Water permeability tests of active films

The water vapor permeability was determined using the infrared sensor technology using a PermatranW3/31 (Mocon, Germany). Samples possessing a surface area of 5 cm^2 were tested at 25 °C. Permeation tests were performed by setting the relative humidity at the downstream and upstream sides of the film to 0% and 50%, respectively. A nitrogen stream flow rate of 100 mL/min was used. Each test was performed in duplicate (Stanzione et al., 2017, p. pp88).

2.4.5. Mechanical properties of composite films

Mechanical tests were performed according to ASTM D882 by using a Lonost Test1 Universal Testing Machine equipped with a 250N load cell and by setting the cross-head speed of 5 mm/min. Five tests were performed for statistical purposes.

2.4.6. Color analysis

The color of the films was determined by using a colorimeter (Minolta Chroma Meter, CR 300, Japan). The Hunter parameters L* (from 0 = black to 100 = white), a* (-a* = greenness to + a* = redness), and b* (- b* = blueness to + b* = yellowness) were measured and averaged from the random positions of each film. The total color difference (ΔE) was calculated according to the following equation (Rhim et al., 1998):

$$\Delta E = \sqrt{\left(L_{film} - L_{standard}\right)^2 + \left(a_{film} - a_{standard}\right)^2 + \left(b_{film} - b_{standard}\right)^2} \quad (1)$$

The film opacity was determined according to the method of Park and Zhao (2004) by measuring the absorbance at 600 nm using the a V-550 UV/VIS spectrophotometer (Jasco, Japan). The films were cut into rectangular pieces (3 cm × 0.4 cm) and placed directly into the cuvette of the spectrophotometer. The results were reported as absorbance divided by film thickness (mm) based on five replicates (Park & Zhao, 2004).

2.4.7. SEM analysis

The morphological analysis of neat and loaded samples was performed by scanning electron microscopy (SEM). In particular, a FEI Quanta 200 FEG scanning electron microscope (ESEM) (FEI, Eindhoven, The Netherlands) in high vacuum mode by using an accelerating voltage within 10–20 kV range and a secondary electron detector (Everhart-Thornley detector) were used.

2.4.8. Extraction of polyphenols from the polymeric matrix

Polyphenols were extracted to determine the total amount of active compounds present in the polymeric matrices that were available for release. Film samples were prepared by cutting three pieces that each possessed a surface area of 6 cm^2. Each piece was immersed in 10 mL of ethanol in a hermetically closed vial and incubated in an oven (ULE400, Memmert GmbH, Germany) at 70 °C for 48 h. Next, the samples were placed in an ultrasonic bath (Branson 5510, Branson Ultrasonic Corp., Danbury, CT, USA) for 4 h at room temperature. Thereafter, the films were removed from the vials, and 2 mL of ethanolic solution was evaporated to dryness under a stream of nitrogen at 40 °C using an evaporator system Labconco Rapid Vertex-Evaporator (Labconco Corporation, Kansas City, MO, USA). Finally, 200 μL of ultra-purified water (Type I) was added to the dry residue and filtered through 0.45 μm PTFE hydrophilic filters prior to chromatographic analysis. All determinations were performed in triplicate.

2.5. Migration assay of active films

Migration analysis was performed to evaluate the release of antioxidant compounds from active films based on the method described by López-de-Dicastillo et al. (2012), with a few changes. The films were cut into 6 cm^2 rectangles, submerged in 10 mL of ethanol 95% (v/v) that acted as the food simulant substitute for fatty foods, according to the European Regulation n° 10/2011 and its amendments (European Commission, 2011), and placed in an oven, for 10 days at 40 °C. At the end of this period, the total content of phenolic compounds and flavonoids released by the active films and also the antioxidant capacity of the active compounds were determied.

For the chromatographic analysis, 4 mL of food simulant was acquired and dried under nitrogen flow at 40 °C (nitrogen obtained from a nitrogen generator Zefiro 40 LC-MS [Clantecnologica, Seville, Spain]). Finally, the residue was redissolved in 200 μL of ultra-purified water, and the final solutions were filtered through 0.45 μm PTFE hydrophilic filters for further HPLC injection. All determinations were performed in triplicate.

2.6. Controlled release assay

To predict the possible inhibition of lipid oxidation over longer periods, two additional controlled release assays were performed. The applied method is described in section 2.5. Migration studies of the films were performed for 10, 20, and 30 days. To evaluate the antioxidant properties, the DPPH assay was performed as described in section 2.9.3.

2.7. Polyphenol identification and quantification via high-performance liquid chromatography with a diode array detector (HPLC-DAD)

Polyphenols were identified and quantified using the methodology described by Andrade et al. (2020) and Barbosa et al. (2021). The analyses were performed using an Agilent HPLC 1200 (Hewlett-Packard, Waldbronn, Germany) equipped with an autosampler, a pump, a degassing system, a thermostatted column system, and a DAD that were all controlled by HP ChemStation software. Phenolic compounds were separated using a reverse-phase Kinetex EVO C18 100 Å column (150 × 3 mm internal diameter, 5 mm of particle size) (Phenomenex, Torrance, CA, USA) at 30 °C.

The mobile phase was composed of two solvents that included water

with 0.1% acetic acid (solvent A) and methanol with 0.1% acetic acid (solvent B). The working gradient was: 0 min, 95% of A, 5% of B; 3 min, 90% of A, 10% of B; 10 min, 80% of A, 20% of B; 18 min, 70% of A, 30% of B; 25 min, 30% of A, 70% of B; 33 min, 0% of A, 100% of B; 33–40 min, 0% of A and 100% of B. Next, the column was returned to initial conditions with 95% A from 40 to 46 min. The mobile phase flow was 0.6 mL/min, and the injection volume was 20 μL. Scanning was performed continuously at wavelengths between 200 nm and 400 nm. The phenolic compounds in the samples were identified comparisons to the retention times and the UV spectrum obtained by the injected standards under the same conditions. Quantification of phenolic compounds was performed using the external standard method incorporating 6-point calibration curves. Stock solutions of the individual standards were prepared in methanol at a concentration of 1000 mg/L. Serial standard solutions were prepared in water by diluting the stock solution at concentration ranges of 0.05–20 mg/L. Each concentration was prepared in triplicate. Quantification was performed at the maximum absorbance of the characteristic wavelengths of the different chemical families of the phenolic compounds (278, 325, and 360 nm).

2.8. Polyphenol identity confirmation by HPLC-ESI-MS/MS

HPLC-ESI-MS/MS (Thermo Fisher Scientific, San José, CA, USA) was used to confirm the presence of phenolic compounds. This instrument was equipped with an Accela quaternary pump, a degassing system, an autosampler, a column, and a TSQ Quantum Access max triple quadrupole mass spectrometer with an electrospray ionization (ESI) source that functioned in positive and negative mode according to the phenolic compounds analyzed. The chromatographic conditions and the column used were the same as those described above for HPLC-DAD analysis.

MS data were acquired in selected reaction monitoring (SRM) mode. Nitrogen gas with a purity of 99.98% was used as the ion sweep gas, envelope, and auxiliary gas, and argon was employed as the collision gas (1.5 mTorr). The MS/MS conditions selected were vaporization temperature set at 340 °C, 2500 V for the electrospray voltage, capillary temperature set at 350 °C, 25 psi of envelope gas, and five arbitrary units of the pressure for the auxiliary gas. The identity of the phenolic compounds was confirmed by comparing the retention time, precursor ion, and fragmentation ions to those obtained from the injection of pure standards.

2.9. Spectrophotometric assays and antioxidant capacity of films

2.9.1. Total polyphenolic content

The total phenolic content (TPC) in the food simulant (ethanol 95%) in contact with the active film (see point 2.5) was quantified by using the method described by Erkan et al. (2008). Briefly, 1 mL of sample was mixed with 7.5 mL of Folin-Ciocalteu reagent (10%, v/v), and after 5 min, this was mixed with 7.5 mL of a sodium carbonate solution (60 mg/mL). The solutions were incubated for 2 h in the dark. At the end of this period, the absorbance was measured at 750 nm using a UV–Vis spectrophotometer Evolution 200 (Thermo Scientific™, Altrincham, England). All analyses were performed in triplicate. Quantification was performed using a calibration curve with gallic acid as the standard. The results of the film migration tests were expressed as μg of gallic acid equivalents per surface area of the film (μg GAE/dm^2). The data for the tomato extracts were expressed in mg of gallic acid equivalents per g of dry weight (mg GAE/g) and are presented in Table S2. Data regarding the lemon extract were described previously by Barbosa et al. (2021).

2.9.2. Total flavonoid content

The total flavonoid content (TFC) in the food simulant (ethanol 95%) in contact with the active film was determined using the method described by Yoo et al. (2008). Briefly, 4 mL of ultrapure water and 0.3 mL of sodium nitrite (5%, w/v) were added to 1 mL of sample. The solutions were homogenized, and after 5 min, 0.6 mL of aluminum chloride (10%, w/v) was added. The solutions were again homogenized, and after 6 min, sodium hydroxide (1 M) and 2.1 mL of ultrapure water were added. The solutions were homogenized, and the absorbance was immediately measured at 510 nm. A calibration curve using epicatechin as a standard was drawn, and the results were expressed in μg of epicatechin equivalents (ECE) per dm^2 (μg ECE/dm^2).

2.9.3. Radical scavenging assay

The determination of the inhibition percentage of the DPPH radical in the food simulant (ethanol 95%) in contact with the active film was performed according to the method initially described by von Gadow et al. (1997) and adapted by Andrade et al. (2018). To 50 μL of the sample, 2 mL of a methanolic solution of DPPH$^{\bullet}$ (14.2 μg/mL) was added, and the solutions were mantained in the dark for 30 min at room temperature (23 ± 1 °C). Next, the absorbance of the solutions was measured at 515 nm using an Evolution 300 UV–Vis spectrophotometer (Thermo Scientific™, England). The inhibition percentage (IP) was calculated using equation (1):

$$IP\ (\%) = \frac{AC - AS}{AC} \times 100. \quad (2)$$

where AC is the absorbance of the blank (water), and AS is the absorbance of the sample.

2.10. Statistical analysis

The films were formulated and further experiments were conducted in triplicate. Statistical data analysis was performed according to a one-way analysis of variance (ANOVA) using IBM® SPSS® Statistics version 26. Tukey's test was used to analyze the differences among mean values. All requirements necessary to perform the ANOVA (normality of data and homogeneity of variances) have been validated. Statistical significance was defined as $p < 0.05$.

3. Results and discussion

3.1. Physical and functional characterization of the active films

The manufactured films were characterized to investigate the effect of LE and TE extracts loading on the chemical structure, thermal stability, diffusion properties, and mechanical behavior of the hosting polymer. The six different active films that were developed in this study are shown in Fig. S1, the color analysis and opacity of the films are reported in Table S1.

3.1.1. Fourier transform infrared spectroscopy (FTIR) of active films

FTIR analysis was performed to study the potential interfacial interactions in LDPE, PLA, and GP composites. For this purpose, FTIR experiments examining LDPE_4LE, LDPE_4 TE, PLA_4LE, PLA_4 TE, GP_4LE, and GP_4 TE composites were performed, and the results were compared to the results of those assessing the neat polymer matrix. FTIR experiments were also performed to assess the natural extracts prior to their inclusion in the polymeric matrices, and the results are presented in Fig. S2 and discussed in the supplementary material section. All spectra are provided in Fig. 1. In the case of the LDPE-based composites (Fig. 1a), the effects of both LE and TE loading were negligible. All spectra exhibit characteristic LDPE bands at 2915 cm^{-1}, 2848 cm^{-1}, 1463 cm^{-1}, and 1377 cm^{-1} that are ascribed to –CH_2 asymmetric, –CH_2 symmetric, stretching deformation, and –CH_3 symmetric bending deformation vibrations, respectively. The frequencies at approximately 729–719 cm^{-1} are related to the deformation vibrations (Doğan et al., 2018).

The spectra for PLA and its composites loaded with lemon and tomato extracts are presented in Fig. 1b. The absorption peaks at 2997 and 2945 cm^{-1} are primarily due to the –CH_2 asymmetric and symmetric

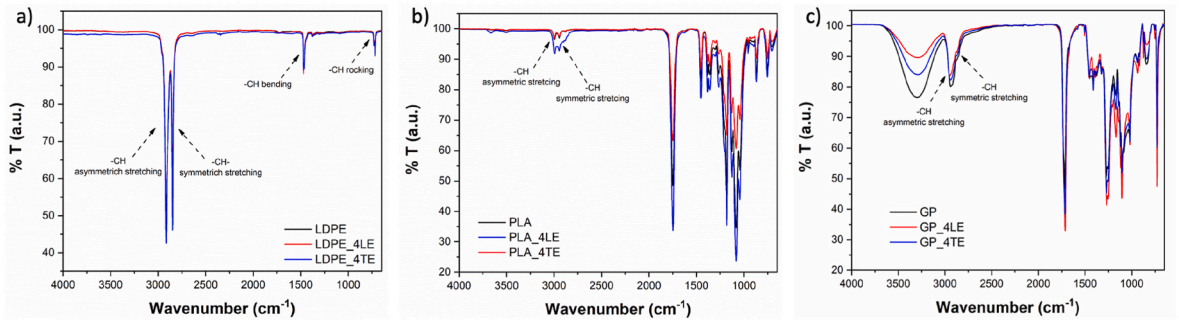

Fig. 1. FTIR spectra for: (a) LDPE, LDPE_4LE, and LDPE_4 TE films; (b) PLA, PLA_4LE, and PLA_4 TE films; (c) GP, GP_4LE, and GP_4 TE films.

vibrations, respectively. A strong absorption band was observed at 1747 cm^{-1} due to C═O stretching from PLA. The bending vibrations within the region 1300–1500 cm^{-1} range are related to the antisymmetric and symmetric deformations of the $–CH_3$ group. The bands at 1266 and 1209 cm^{-1} are ascribed to the C–O–C antisymmetric and symmetric stretching in esters, and the peak at 1180 cm^{-1} could be attributed to the C–O–C stretching of PLA. The three peaks, respectively at 1,125, 1,080, and 1040 cm^{-1} may correspond to C–O stretching vibrations. The last two bands detected at 868 and 755 cm^{-1} (far infrared) can be assigned to the amorphous and crystalline phases of PLA, respectively (Pamuła et al., 2001). The presence of LE did not significantly affect the chemical behavior of PLA. In contrast, the TE addition led to an intensification of all PLA characteristic peaks, and this was likely related to the presence of the natural extract –C═O and $–CH_2$ functional groups.

The neat GP and the GP-based active film highlight all major peaks related to the hydroxyl and acetate groups (Fig. 1c). The large bands observed between 3550 and 3000 cm^{-1} are related to –OH stretching arising from the intermolecular and intramolecular hydrogen bond networks. Furthermore, absorption bands that are ascribed to –OH vibration and H–OH bending of absorbed water molecules may also be present in this region due to the high GP hydrophilicity (Wang et al., 2020). The peaks at 2,940, 2,910, 1425 and 1329 cm^{-1} are ascribed to the $–CH_2$ groups asymmetric and symmetric stretching, $–CH_2$ bending vibration, and –CH deformation respectively. The peak at 1720 cm^{-1} is due to the C═O stretching from acetate groups (Peresin et al., 2010), whereas the two peaks at 1114 cm^{-1} and approximately 1080 cm^{-1} are assigned to the C–C stretching vibrations of the polymeric chain in the crystalline phase. The loading of TE and LE into the polymeric matrix reduced the peak intensity in the region between 3500–3000 cm^{-1} in a relevant manner. The decrease in the absorbance intensity of the –OH band in this region could be likely related to the relevant amount of highly reducing agents such as ascorbic acid and superoxide free radical scavengers that may have led to a reduction in the hydroxyl group concentration as indicated by the FTIR spectra (Kannat et al., 2017; Wang et al., 2020).

3.1.2. *Thermal analysis (TGA and DSC) of composite films*

Thermal stability in terms of degradation, crystallinity, and glass transition, of neat LDPE, PLA, GP, and the resulting composites was studied using TGA and DSC. Fig. 2 presents the temperature-dependent mass loss behavior of the three different polymers and the corresponding loaded systems. A single degradation step was used to characterize the LDPE and LDPE-based composites. Both LDPE and LDPE_4LE exhibited similar maximum degradation rates (Fig. 2a). Conversely, TE loading into the LDPE matrix shifts the maximum degradation rate toward higher temperatures compared to those of the neat polymer curve (blue curve in Fig. 2a). TE addition could, as a consequence of the melt mixing process, likely induce a contact-by-contact structural configuration between filler particles and macromolecules, thus leading to an effective reduction of the molecular weight of the hosting polymer and a consequent higher volatility of the blends that is clearly reflective of the thermal stability of the final system and also the mechanical data. It is reasonable to assume that the molecular length of the polymer is reduced, thus leading to a higher stability, and that the presence of contact will reflect the lower modulus and elongation at break for the final composite films (Fig. 3) (Yusof et al., 2018; Suñer et al., 2015). Neat PLA (black curve in Fig. 2b) undergoes a single-step degradation process with the main degradation peak at around 370 °C, and the incorporation of LE into the PLA matrix slightly decreased the thermal properties of the resulting composite. The TE addition induced a lower thermal stability of the resulting composite, thus reducing the maximum temperature of the degradation rate. The addition of both LE and TE led to a decrease in the cold crystallization temperature (Tc) of the resulting composites. This phenomenon is more evident in the experiment involving the TE filler and could be ascribed to both the increased chain mobility that enables PLA to crystallize at lower temperatures upon cooling and the TE plasticizing effect that was confirmed by the attained mechanical performance (see Fig. 3 and Table 2) (Kang et al., 2018). In the case of the GP composites (Fig. 2c), the effect of both loading extracts was negligible. Indeed, all the curves are characterized by two degradation step mechanisms and exhibit a maximum degradation rate at 342.8 °C and 407.0 °C, respectively.

The DSC thermograms were analyzed, and the main characteristic

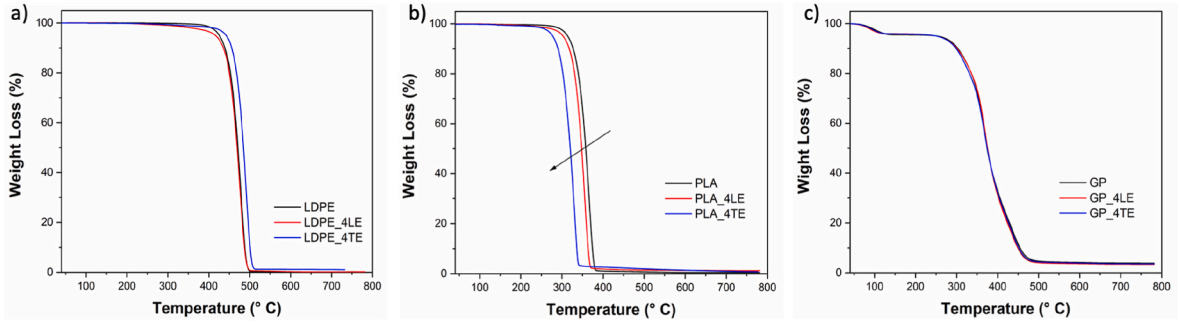

Fig. 2. TGA curves for: (a) neat and LDPE-based composites; (b) neat and PLA-based composites; (c) neat and GP-based composites.

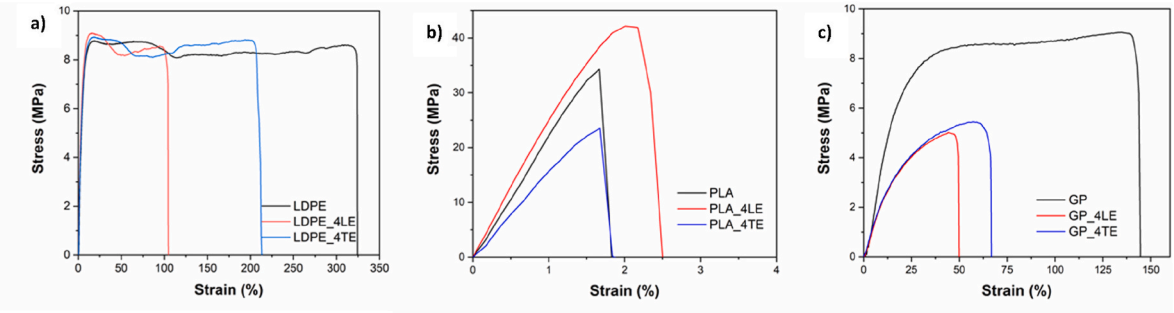

Fig. 3. Stress vs strain cuves for: (a) LDPE, LDPE_4LE, and LDPE_4 TE films; (b) PLA, PLA_4LE, and PLA_4 TE films; (c) GP, GP_4LE, and GP_4 TE films.

parameters related to the second scan are listed in Table 1.

Analysis of the DSC data reveals that the effect of filler is relevant regarding GP but is not substantial in the case of PLA and LDPE. For the GP matrix, the glass transition temperature is reduced from 85 °C to 77 °C, thus supporting the conclusion that a plasticization phenomenon occurred.

3.1.3. Contact angle measurements and water permeability of composite films

The influence of LE and TE on the barrier properties of the active films was investigated by measuring of water vapor permeability and also the hydrophobicity of their surfaces through the use of contact angle analysis. The contact angle images and water permeability results for LDPE, PLA, and GP and for the respective neat films are presented in Fig. 4.

It can be observed that the addition of LE to the LDPE matrix does not significantly affect its water permeability, whereas the addition of TE leads to an increase in the water permeability of approximately one order of magnitude compared to that of the neat polymer (Fig. 4a). For the other polymer matrices, we observed in both cases that the addition of LE leads to a decrease in water permeability of approximately 44.6% and 34.8%, respectively, for the GP and PLA. For the TE loading, this decrease was approximately 22.0% and 12.2%, respectively.

Wettability measurements revelead that the hydrophilic features of the neat polymers of LDPE and GP were not modified by the presence of the extracts, as the contact angle values changed only within the experimental error range. A significant variation was observed only for the PLA_4LE film that exhibits an increase in the surface hydrophilicity (contact angle value of approximately 78°). Thus, it is likely that the observed water barrier improvement can be ascribed not to a solubility reduction related to a more hydrophobic surface and instead to diffusivity reduction that is likely due to a crosslinking effect that is evidenced by the mechanical properties behavior.

3.1.4. Mechanical properties of composite films

Mechanical characterization in the tensile configuration was performed to analyze the induced effect of LE and TE on the macroscopic behavior of LDPE, PLA, and GP-based composite films compared to the behavior of neat films. Table 2 reports the averaged values and corresponding standard deviations for the Young Modulus, Stress and Elongation at break of five samples. For completeness purpose, the trend of the mechanical behavior of all neat and composite films are reported in Fig. 3 as the stress-strain curve of one single tested sample chosen among the five tested for each typology. From the obtained data it can be noted that the presence of both LE and TE filler within each matrix causes an embrittlement of the neat system, thus reducing the maximum extension at failure by approximately 65%, 30%, and 60%, respectively, for LDPE-, PLA- and GP-based composite films containing LE and approximately 50%, 15%, and 26% for the same films containing TE extract. This is likely due to a crosslinking formation between the phenolic compounds and the polymer matrices that hinder the intramolecular mobility and thus create a more rigid structure (Menzel et al., 2020; Stanzione et al., 2021). It has been demonstrated that the failure is almost unaffected in the case of LDPE films, is slightly reduced (approximately 10%) in the case of PLA_4LE, and is reduced by approximately 40%, 46%, and 30% in the cases of PLA/TE, GP/LE, and GP/TE, respectively. The major relevant effect is related to the presence of the plateau that was observed in the case of GP and that completely disappeared in the films containing both fillers. For the Young modulus values of the samples that were tested, this value was reduced by approximately 40%, 51%, and 46% in the cases of LDPE/LE GP/LE, and GP_4 TE, respectively, and it remained unchanged or affected within the experimental error in the cases of LDPE_4 TE, PLA_4LE, and PLA_4 TE, respectively. The obtained results reveal that the mechanical properties of PLA-based films remain predominantly unaffected by the presence of the active extracts. In order to assess the roughness induced by the manufacturing process and to investigate characteristic failure modes to be correlated with the analysis of mechanical tests, SEM analysis was also performed, on both the surface and the cross section of tested samples. SEM images are reported in Fig. S3 and morphological analysis is discussed in the SI section.

Table 1
DSC (second scan) parameters of neat LDPE, PLA, GP and corresponding active films prepared with extracts from tomato and lemon by-products.

	T_g (°C)	T_{cold} (°C)	ΔH_{cold} (J/g)	T_m (°C)	ΔH_m (J/g)
LDPE	-	-	-	109.9	100.9
LDPE_4LE	-	-	-	110.3	130.3
LDPE_4 TE	-	-	-	111.6	124.9
PLA	60.9	111.9	35.3	167.2	43.7
PLA_4LE	58.8	103.4	36.4	165.1	51.6
PLA_4 TE	60.5	107.1	35.9	165.7	40.7
GP	85.3	-	-	-	-
GP_4LE	77.9	-	-	-	-
GP_TE	76.4	-	-	-	-

Tg - glass transition temperature; Tcold - crystallization temperature; ΔHcold - crystallization enthalpy; Tm - melting temperature; ΔHm - melting enthalpy.

Table 2
Measured parameters from mechanical tensile tests of neat LDPE, PLA, GP and the respective active films.

	Stress at break (MPa)	Elongation at break (%)	Young Modulus (MPa)
LDPE	9.3 ± 0.6 ^{c}	367.8 ± 48.4 ^{a}	175.0 ± 7.4 ^{d}
LDPE_4LE	8.9 ± 0.7 ^{c}	130.4 ± 25.3 ^{c}	104.2 ± 8.1 ^{d}
LDPE_4 TE	9.0 ± 0.5 ^{c}	192.1 ± 38.3 ^{b}	158.1 ± 5.4 ^{d}
PLA	36.3 ± 3.5 ^{a}	1.9 ± 0.3 ^{f}	1957.4 ± 166.8 ^{c}
PLA_4LE	39.8 ± 5.8 ^{a}	2.7 ± 0.4 ^{f}	2206.4 ± 218.7 ^{b}
PLA_4 TE	24.3 ± 2.3 ^{b}	2.3 ± 0.2 ^{f}	1410.4 ± 260.7 a
GP	8.8 ± 0.4 ^{c}	128.7 ± 15.7 ^{c}	43.5 ± 4.7 ^{d}
GP_4LE	4.7 ± 0.7 ^{d}	52.4 ± 8.8 ^{e}	21.1 ± 1.7 ^{d}
GP_4 TE	6.0 ± 0.3 ^{cd}	64.1 ± 13.3 ^{d}	22.9 ± 3.2 ^{d}
Sig.	***	***	***

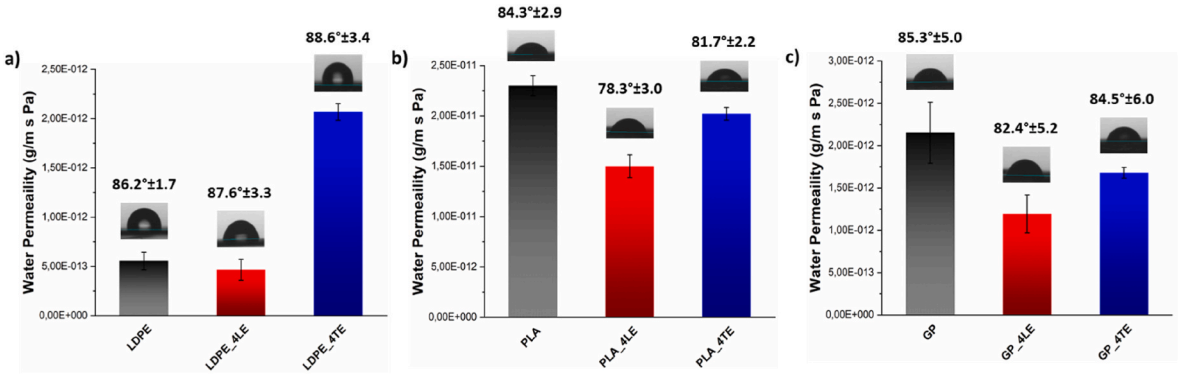

Fig. 4. Water Permeability data and contact angle images incorporating statistical values for the mean and standard deviation for: (a) LDPE, LDPE_4LE, and LDPE_4 TE films; (b) PLA, PLA_4LE, and PLA_4 TE films; (c) GP, GP_4LE, and GP_4 TE films.

3.1.5. *Polyphenolic profiles and contents of films and migration results*

Table 3 displays the phenolic compounds that were identified and confirmed using HPLC-ESI-MS/MS. Each compound was characterized according to its retention time (Rt), maximum absorption wavelength (λ_{max}), structural class, molecular formula, molecular ion, and main MS/MS fragments. A total of 11 phenolic compounds were identified in the lemon-based films, whereas in the tomato-based films, there were seven compounds. Phenolic acids such as protocatechuic, caffeic, *p*-coumaric, and chlorogenic acids and the flavonoids rutin, naringenin, and quercitrin were identified in films produced with both extracts. In contrast, 4-hydroxybenzoic acid, ferulic acid, eriocitrin, and hesperidin were detected in lemon-based films. The polyphenolic profiles are in agreement with those observed for lemon and tomato by-products that were described previously in the literature (Barbosa et al., 2021; Tamasi et al., 2019; Vallverdú-Queralt et al., 2011).

Table S3 summarizes the parameters for detection and quantification of the phenolic compounds by HPLC-DAD, including the maximum absorption wavelengths (λ_{max}), linearity, LOD, and LOQ analysis, and the standard curves. Fig. S4 presents the chromatograms that were acquired at 278 nm for one replicate of each sample film from HPLC-DAD, and the results from the extraction and migration assays are provided in Table 4.

All phenolic compounds identified in LDPE_4 TE by mass spectrometry were at levels below the LOQ. Conversely, for PLA_4 TE, the polyphenols caffeic acid, *p*-coumaric acid and chlorogenic acid were quantified, and the latter was observed at higher concentrations (18 μg/dm^2). For the GP_4 TE film, the compounds protocatechuic acid, chlorogenic acid, rutin and naringenin were quantified. The most abundant compounds in this film were naringenin, rutin, and they reached concentrations of approximately 10 μg/dm^2 (Table 4). These results are in agreement with those previously described in the literature by Ćetković et al. (2012) for tomato wastes, where naringenin and rutin were found in higher amounts.

Among the compounds identified by mass spectrometry in LDPE_4LE, 4-hydroxybenzoic acid, *p*-coumaric acid, quercitrin, and naringenin were quantified by HPLC-DAD. 4-hydroxybenzoic acid was present at the highest concentration (10 μg/dm^2). In PLA_4LE, the compounds that were quantified were 4-hydroxybenzoic acid, chlorogenic acid, *p*-coumaric acid, ferulic acid, eriocitrin, hesperidin, rutin, and naringenin. From these, eriocitrin and hesperidin were present in higher amounts at concentrations of 79 and 85 μg/dm^2, respectively. These flavonoids were previously described as the major phenolics that were onbserved in lemon by-products by Barbosa et al. (2021). GP_4LE, 4-hydroxybenzoic acid, eriocitrin, hesperidin, quercitrin, and naringenin were quantified. Additionally, eriocitrin and hesperidin were present at high concentrations (164 and 109 μg/dm^2, respectively).

Among all the active films that were formulated, the LDPE polymers exhibited the lowest capacity to release phenolic compounds. In contrast, PLA and GP possessed 7 to 15-folds higher release rates. These differences could be due to the low diffusion coefficient of LDPE that is related to the molecular structure of the active compounds and, thus, their capacity to be liberated. (GilakHakimabadi et al., 2019; Wang & Rhim, 2016).

Considering the dataset from all lemon-based films presented in Table 4, GP_4LE displayed the highest migration percentage (65.0%), and this was followed by PLA_4LE (30.7%) and LDPE_4LE (4.4%). Among the phenolic compounds, 4-hydroxybenzoic and naringenin exhibited favorable migration from all films. Eriocitrin and hesperidin were the most abundant compounds in GP_4LE and PLA_4LE.

The films formulated with lemon extract released high amounts of individual and total phenolic compounds to the food simulant in the specific migration assay. These differences were also observed in the ethanolic solution obtained from the complete extraction assay of the different polymeric matrices. Even though the amount of the lemon and tomato extracts included in the films were the same, the results confirmed that the nature of the polymeric matrix might interfere with the availability of the extractable active compounds. Thus, the migration of the active compounds also depends upon the polymeric matrix, where GP is the most suitable for polyphenols release.

3.2. *Antioxidant capacity and total phenolics and flavonoids contents*

As anticipated, neat PLA, LDPE, and GP did not inhibit the DPPH radical (Table 5). The PLA_4 TE presented the highest DPPH$^{\bullet}$ IP (9.10 ± 0.25%), and this was followed by the GP_4 TE, GP_4LE, and PLA_4LE (4.55 ± 0.67%, 4.35 ± 0.17% and 4.24 ± 0.32%, respectively). This high antioxidant capacity of tomato extract could be due to the presence of the hydroxycinnamic acids (caffeic acid and chlorogenic acid) that were identified and quantified by HPLC (Table 4, Fig. S4). The PLA_4 TE also exhibited the highest content of phenolic compounds (5004.9 ± 4.5 μg GAE/dm^2), and this was followed by the GP_4 TE (4860.6 ± 38.2 μg GAE/dm^2), GP_4LE (4545.8 ± 24.9 μg GAE/dm^2), and PLA_4LE (4073.7 ± 140.5 μg GAE/dm^2). For the neat PLA, LDPE, and GP, lower responses to and in the spectrophotometric assays were also observed, and these responses were likely due to the presence of other compounds possessing –OH groups that were present in the polymer. Regarding the total content in flavonoids, the PLA_4LE exhibited the highest value (5672.2 ± 395.8 μg ECE/dm^2), and this was followed by the GP_4LE (3464.0 ± 182.8 μg ECE/dm^2) and the GP_4 TE (2855.3 ± 183.2 μg ECE/dm^2). These results were in agreement with the HPLC data, as the main compounds quantified in these films were flavanone and flavonol glycosides (Table 4).

It is evident that the PLA and GP films present a higher migration than do the LDPE films, thus confirming that they are more suitable polymers for use in active packaging systems.

Although the radical scavenging assay values for the PLA and GP active films were similar, except for PLA_4 TE that was higher, in general

Table 3
Phenolic compounds identified in the active films by HPLC-DAD and confirmed by HPLC-ESI-MS/MS.

#	Compound	λ_{max}	R_t (min)	Molecular formula	$[M–H]^-$ m/z	Main MS/MS fragments (m/z)	Structural subclass	Tomato			Lemon		
								LDPE_4 TE	PLA_4 TE	GP _4 TE	LDPE_4LE	PLA_4LE	GP_4LE
1	Protocatechuic acid	260–293	4.31	$C_7H_6O_4$	153.0	108, 109	Benzoic acid derivates	×	✓	✓	✓	✓	✓
2	4-hydroxybenzoic acid	255	7.09	$C_7H_6O_3$	136.7	93, 65	Benzoic acid derivates	×	×	×	✓	✓	✓
3	Caffeic acid	245/325	9.59	$C_9H_8O_4$	179	134, 135	Hydroxycinnamic acids	✓	✓	✓	×	✓	✓
4	Chlorogenic acid	250/325	9.99	$C_{16}H_{18}O_9$	353.0	191	Cinnamic acids	✓	✓	✓	✓	✓	✓
5	*p*-coumaric acid	310/325	13.39	$C_9H_8O_3$	163	93, 119	Hydroxycinnamic acids	✓	✓	✓	✓	✓	✓
6	Ferulic acid	245/325	15.26	$C_{10}H_{10}O_4$	193.0	134	Hydroxycinnamic acids	×	×	×	×	✓	×
7	Eriocitrin	285	17.95	$C_{27}H_{32}O_{15}$	595	449	Flavanone glycosides	×	×	×	×	✓	✓
8	Hesperidin	290/355	21.36	$C_{28}H_{34}O_{15}$	609	301	Flavanone glycosides	×	×	×	×	✓	✓
9	Rutin	255/360	21.58	$C_{27}H_{30}O_{16}$	609.1	299, 270	Flavonoid glycosides	✓	✓	✓	✓	✓	×
10	Quercitrin	250/350	22.5	$C_{21}H_{20}O_{11}$	447	300, 285	Flavonoid glycosides	✓	✓	✓	✓	✓	✓
11	Naringenin	295	23.71	$C_{15}H_{12}O_5$	270.9	119, 151	Flavonoid glycosides	✓	✓	✓	✓	✓	✓

R_t–retention time; λ_{max}–maximum absorption wavelengths; $[M–H]^-$–molecular ions; ✓–indicates the presence of the compound identified; × –indicates the absence of the phenolic compound.

the PLA films exhibited improved properties. However, considering the appearance of the films, those containing tomato extract possessed a more intense brown colour compared to the color of those containing lemon by-product extract (see Fig. S1), and this may represent a limitation considering the consumer acceptance of the hypothetical final incorporation of these films into the market as active packaging. Thus, to consider and balance the water barrier and mechanical results of the PLA_4 TE sample, the films prepared with the lemon by-product extract (PLA_4LE) were selected as the most suitable for further investigation.

To evaluate the stability and possible inhibition of lipid oxidation, the antioxidant capacity of PLA that was supplemented with 4% of lemon by-product extract (PLA_4LE) was also tested after 20 and 30 days of contact with the food simulant (95% ethanol) at 40 °C. As presented in Fig. 5, the active compounds of the active film gradually migrate to the simulant and still possess some radical scavenging activity even after 30 days at 40 °C, thus indicating that the lemon extract is somehow preserved and protected by the PLA film. This gradual migration can be useful for preserving fatty foods, as lipid oxidation will gradually increase with storage time. Based on the results obtained in this study and the antioxidant activity and the TPC and TFC content of the isolated extracts, the packages incorporated with the lemon by-product extracts appear to be the most useful for packing fatty foods with high percentages of unsaturated lipids, as they are the most susceptible to lipid oxidation.

4. Conclusions

Three different polymeric matrices (LDPE, PLA, and GP) were loaded with extracts yielded from lemon and tomato by-products generated during industrial juice processing.

The FTIR analysis indicated that the use of LE and TE fillers may lead to chemical changes in the structure of the neat polymeric matrices (primarily in PLA- and GP-based composites) due to the interactions with the –OH groups of TE and LE polyphenols.

The crosslinking effect of the polymer matrix lead to a substantial improvement in water barrier properties for PLA and GP-based films containing LE and TE.

The overall embrittlement associated with TE filler in the PLA and GP matrices was not observed for the LDPE films. The PLA-based films were those possessing mechanical properties that remain slightly affected by the presence of the active extracts.

GP and PLA are the polymeric matrices that have been demonstrated to be the most suitable for releasing phenolic compounds with high antioxidant capacity, and thus, they possess high potential for use in active packaging. Hesperidin and eriocitrin were the most important compounds in lemon extract films. Protocatechuic acid and chlorogenic acid were the primary compounds in the tomato films. The specific migration assay suggested that PLA_4LE was the best film to release high amounts of phenolic compounds (predominantly flavonoids). Further studies are required to evaluate the effectiveness of active films containing lemon by-product extracts in regard to inhibiting the lipid oxidation of foods possessing high lipid content.

Funding

This work was carried out in the frame of the VIPACFood project (grant agreement no. 618127). This project was funded by ARIMNet2 (Coordination of Agricultural Research in the Mediterranean; 2014–2017), an ERA-NET Action financed by the European Union under the 7th Framework Programme. In Spain this action was co-funded by the Spanish National Institute for Agricultural and Food Research and Technology (MINECO-INIA) ref. APCIN2016-00061-00-00.

CRediT authorship contribution statement

Sandra Mariño-Cortegoso: Data curation, Formal analysis,

Table 4
Total concentration of the different phenolic compounds presents in the films and concentrations determined by specific migration assay with HPLC-DAD and expressed as μg/dm^2 film.

Compound	Assay	Lemon extract			Sig.	Tomato extract			Sig.
		GP	PLA	LDPE		GP	PLA	LDPE	
Protocatechuic acid	Extraction	<LOQ	<LOQ	<LOQ		10.45 ± 0.92	<LOQ	–	
	Migration	<LOQ	<LOQ	<LOQ		5.40 ± 0.79 ^{B}	<LOQ	–	
4-hydroxybenzoic acid	Extraction	13.59 ± 0.50 ^{cdß}	20.70 ± 1.11 ^{bα}	10.10 ± 0.64 ^{aγ}	***	–	–	–	
	Migration	10.16 ± 1.78 ^{C}	11.58 ± 0.62 ^{C}	9.97 ± 0.32 ^{A}	n.s.	–	–	–	
Caffeic acid	Extraction	<LOQ	<LOQ	–		<LOQ	10.09 ± 3.86 ^{b}	<LOQ	
	Migration	<LOQ	<LOQ	–		<LOQ	5.19 ± 3.17	<LOQ	
Chlorogenic acid	Extraction	<LOQ	7.94 ± 0.95 ^{d}	<LOQ		9.96 ± 0.25 ^{ß}	18.11 ± 0.39 ^{aα}	<LOQ	***
	Migration	<LOQ	<LOQ	<LOQ		3.17 ± 0.31 ^{C}	3.50 ± 2.24	<LOQ	n.s.
p-coumaric acid	Extraction	<LOQ	11.78 ± 1.80 ^{cdα}	3.71 ± 0.55 ^{cß}	***	<LOQ	2.58 ± 0.15 ^{c}	<LOQ	
	Migration	<LOQ	7.72 ± 0.32 ^{Dα}	2.22 ± 0.95 ^{Cß}	***	<LOQ	<LOQ	<LOQ	
Ferulic acid	Extraction	–	10.59 ± 2.58 ^{cd}	–		–	–	–	
	Migration	–	0.25 ± 0.01 ^{F}	–		–	–	–	
Eriocitrin	Extraction	164.68 ± 4.60 ^{aα}	79.04 ± 1.25 ^{aß}	–	***	–	–	–	
	Migration	124.21 ± 24.00 ^{Aα}	31.85 ± 1.25 ^{Bß}	–	***	–	–	–	
Hesperidin	Extraction	109.03 ± 4.53 ^{bα}	85.31 ± 9.07 ^{aß}	–	**	–	–	–	
	Migration	90.07 ± 18.48 ^{Bα}	55.97 ± 0.83 ^{Aß}	–	*	–	–	–	
Rutin	Extraction	–	8.02 ± 0.28 ^{d}	<LOQ		11.66 ± 0.53	<LOQ	<LOQ	
	Migration	–	<LOQ	<LOQ		15.63 ± 0.38 ^{A}	<LOQ	<LOQ	
Quercitrin	Extraction	15.62 ± 0.30 ^{cα}	<LOQ	4.95 ± 2.13 ^{bcß}	***	<LOQ	<LOQ	<LOQ	
	Migration	9.80 ± 2.29 ^{C}	<LOQ	<LOQ		<LOQ	<LOQ	<LOQ	
Naringenin	Extraction	9.16 ± 0.48 ^{dß}	16.71 ± 3.88 ^{bcα}	7.49 ± 1.77 ^{abß}	**	10.92 ± 1.66	<LOQ	<LOQ	
	Migration	4.68 ± 1.49 ^{C}	4.96 ± 2.35 ^{E}	3.77 ± 0.16 ^{B}	n.s.	<LOQ	<LOQ	<LOQ	
Sig.	Extraction	***	***	**		n.s.	***	n.a.	
	Migration	***	***	***		***	n.s.	n.a.	

Statistical significance: ***$p < 0.001$; **$p < 0.01$; *$p < 0.05$; and n.s. = not significant ($p > 0.05$). Different capital letters show the statistical significance among the migration dataset for the three polymeric matrices, while the lowercase letters display the differences among the extraction data obtained for the several films prepared with lemon or tomato byproducts extracts. On the other hand, different Greek letters displayed the statistical significance among the phenolic compounds quantified within the same film after the extraction process of the films. n.a., not applicable; LOQ, Limit of quantification.

Table 5
Results for the DPPH radical inhibition assay and the determination of the Total Phenolic Content of the migration assays, presented in μg of Gallic Acid Equivalents per dm^2, and the Total Flavonoids Content presented in μg of Epicatechin Equivalents per dm^2. The results are presented as mean ± SD of three replicates.

Film sample	DPPH$^{\bullet}$ Inhibition Percentage (%)	TPC (μg GAE/dm^2)	TFC (μg ECE/dm^2)
LDPE	0.64 ± 0.2 ^{ad}	3070.2 ± 8.8 ^{ac}	1671.9 ± 282.5 ^{abc}
LPDE_4LE	0.99 ± 0.09 ^{ab}	3467.8 ± 16.3 ^{f}	1890.2 ± 74.6 ^{abc}
LDPE_4 TE	1.46 ± 0.16 ^{b}	3264.1 ± 58.5 ^{b}	1353.5 ± 201.5 ^{c}
PLA	0.00 ± 0.0^{d}	2994.2 ± 12.7 ^{c}	1645.9 ± 120.0 ^{abc}
PLA_4LE	4.24 ± 0.32 ^{c}	4073.7 ± 140.5 ^{e}	5672.2 ± 395.8 ^{f}
PLA_4 TE	9.10 ± 0.25 ^{e}	5004.9 ± 4.5 ^{d}	1968.3 ± 206.4 ^{abc}
GP	0.51 ± 0.41 ^{ad}	3193.0 ± 23.9 ^{ab}	2260.6 ± 273.6 ^{abde}
GP_4LE	4.35 ± 0.17 ^{c}	4545.8 ± 24.9 ^{g}	3464.0 ± 182.8 ^{e}
GP_4 TE	4.55 ± 0.67 ^{c}	4860.6 ± 38.2 ^{d}	2855.3 ± 183.2 ^{de}

Different superscript lower-case letters denote significant differences ($p < 0.05$) among samples by Tukey's test.

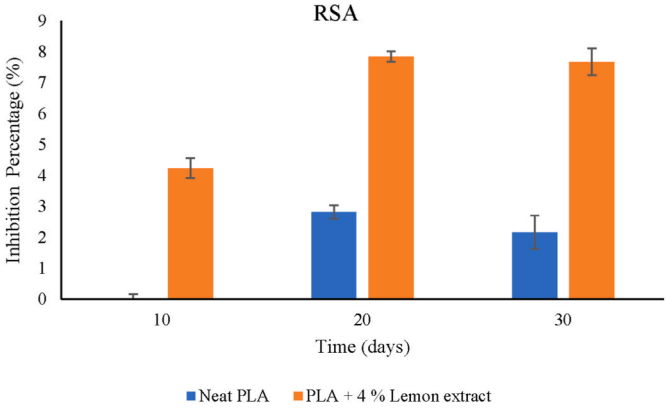

Fig. 5. DPPH scavenging activity of the food simulant (ethanol 95%) in contact with the PLA and PLA_4LE films at a maximum storage time of 30 days at 40 °C.

Investigation, Methodology, Writing – original draft. **Mariamelia Stanzione:** Formal analysis, Writing – original draft, Investigation, Methodology. **Mariana A. Andrade:** Conceptualization, Formal analysis, Methodology, Writing – original draft. **Cristina Restuccia:** Funding acquisition, Project administration, Resources. **Ana Rodríguez-Bernaldo de Quirós:** Conceptualization, Data curation. **Giovanna G. Buonocore:** Funding acquisition, Project administration, Resources, Supervision, Writing – review & editing. **Cássia H. Barbosa:** Formal analysis. **Ana Sanches Silva:** Funding acquisition, Project administration, Resources, Supervision, Writing – review & editing. **Fernando Ramos:** Funding acquisition, Project administration, Resources. **Khaoula Khwaldia:** Funding acquisition, Project administration, All authors have read and agreed to the published version of the manuscript. **Raquel Sendón:** Conceptualization, Funding acquisition, Project administration, Resources, Supervision, Writing – review & editing. **Letricia Barbosa-Pereira:** Conceptualization, Data curation, Investigation, Methodology, Software, Supervision, Validation, Writing – review & editing.

Acknowledgments

L. Barbosa-Pereira is grateful to the Spanish Ministry of Science,

Innovation and Universities for her "Juan de la Cierva-Incorporación" Grant (Agreement No. IJCI-2017-31665). C. H. Barbosa is grateful for her research grant in the frame of the VIPACFood project (ARIMNET2/0003/2016) and for the Ph.D. Grant 2021.08154.BD from the Fundação para a Ciência e Tecnologia (FCT), Portugal. Technical support of Mrs A. Aldi for film characterization is also kindly acknowledged.

Appendix A. Supplementary data

Supplementary data to this article can be found online at https://doi.org/10.1016/j.foodcont.2022.109128.

References

Adilah, A. R., Jamilah, B., Noranizan, M. A., & Hanani, Z. A. N. (2018). Utilization of mango peel extracts on the biodegradable films for active packaging. *Food Packaging and Shelf Life, 16*, 1–7. https://doi.org/10.1016/j.fpsl.2018.01.006

Andrade, M. A., de Oliveira Torres, L. R., Silva, A. S., Barbosa, C. H., Vilarinho, F., Ramos, F., de Quirós, A. R. B., Khwaldia, K., & Sendón, R. (2020). Industrial multi-fruits juices by-products: Total antioxidant capacity and phenolics profile by LC–MS/MS to ascertain their reuse potential. *European Food Research and Technology, 246*(11), 2271–2282. https://doi.org/10.1007/s00217-020-03571-3

Andrade, M. A., Ribeiro-Santos, R., Costa Bonito, M. C., Saraiva, M., & Sanches-Silva, A. (2018). Characterization of rosemary and thyme extracts for incorporation into a whey protein-based film. *LWT – Food Science and Technology, 92*(January), 497–508. https://doi.org/10.1016/j.lwt.2018.02.041

Barbosa-Pereira, L., Angulo, I., Lagarón, J. M., Paseiro-Losada, P., & Cruz, J. M. (2014). Development of new active packaging films containing bioactive nanocomposites. *Innovative Food Science & Emerging Technologies, 26*, 310–318. https://doi.org/10.1016/j.ifset.2014.06.002

Barbosa, C. H., Andrade, M. A., Séndon, R., Silva, A. S., Ramos, F., Vilarinho, F., Khwaldia, K., & Barbosa-Pereira, L. (2021). Industrial fruits by-products and their antioxidant profile: Can they Be exploited for industrial food applications? *Foods, 10*(2), 272. https://doi.org/10.3390/foods10020272

Carocho, M., Barreiro, M. F., Morales, P., & Ferreira, I. C. (2014). Adding molecules to food, pros and cons: A review on synthetic and natural food additives. *Comprehensive Reviews in Food Science and Food Safety, 13*(4), 377–399. https://doi.org/10.1111/1541-4337.12065

Ćetković, G., Sladjana Savatović, S., Čanadanović-Brunet, J., Djilas, S., Vulić, J., Mandić, A., & Četojević-Simin, D. (2012). Valorisation of phenolic composition, antioxidant and cell growth activities of tomato waste. *Food Chemistry, 133*, 938–945. https://doi.org/10.1016/j.foodchem.2012.02.007

Doğan, F., Şirin, K., Kolcu, F., & Kaya, İ. (2018). Conducting polymer composites based on LDPE doped with poly (aminonaphthol sulfonic acid). *Journal of Electrostatics, 94*, 85–93. https://doi.org/10.1016/j.elstat.2018.07.004

Erkan, N., Ayranci, G., & Ayranci, E. (2008). Antioxidant activities of rosemary (Rosmarinus Officinalis L.) extract, blackseed (Nigella sativa L.) essential oil, carnosic acid, rosmarinic acid and sesamol. *Food Chemistry, 110*(1), 76–82. https://doi.org/10.1016/j.foodchem.2008.01.058

European Commission. (2011). Commission Regulation (EU) No 10/2011 of 14 January 2011 on plastic materials and articles intended to come into contact with food. *Official Journal of the European Union, 12*, 1–89. https://eur-lex.europa.eu/legal-content/EN/ALL/?uri=CELEX%3A32011R0010.

European Commission. Eurostat. (2021). https://ec.europa.eu/info/sites/default/files/food-farming-fisheries/farming/documents/citrus-dashboard_en.pdf, 13 January 2022.

European Commission. Eurostat. (2022). https://ec.europa.eu/info/sites/default/files/food-farming-fisheries/farming/documents/tomato-dashboard_en.pdf, 13 January 2022.

Faustino, M., Veiga, M., Sousa, P., Costa, E. M., Silva, S., & Pintado, M. (2019). Agro-food byproducts as a new source of natural food additives. *Molecules, 24*(6), 1056. https://doi.org/10.3390/molecules24061056

Fiorentini, C., Garrido, G. D., Bassani, A., Cortimiglia, C., Zaccone, M., Montalbano, L., Martinez-Nogues, V., Cocconcelli, P. S., & Spigno, G. (2022). Citrus peel extracts for industrial-scale production of bio-based active food packaging. *Foods, 11*, 30. https://doi.org/10.3390/foods11010030

von Gadow, A., Joubert, E., & Hansmann, C. F. (1997). Comparison of the antioxidant activity of aspalathin with that of other plant phenols of rooibos tea (Aspalathus linearis), a-tocopherol, BHT, and BHA. *Journal of Agricultural and Food Chemistry, 45*(3), 632–638. https://doi.org/10.1021/jf960281n

Giannakas, A., Salmas, C., Leontiou, A., Tsimogiannis, D., Oreopoulou, A., & Braouhli, J. (2019). Novel LDPE/chitosan rosemary and melissa extract nanostructured active packaging films. *Nanomaterials, 9*(8), 1105. https://doi.org/10.3390/nano9081105

GilakHakimabadi, S., Ehsani, M., Khonakdar, H. A., Ghaffari, M., & Jafari, S. H. (2019). Controlled-release of ferulic acid from active packaging based on LDPE/EVA blend: Experimental and modeling. *Food Packaging and Shelf Life, 22*, Article 100392. https://doi.org/10.1016/j.fpsl.2019.100392

Gowe, C. (2015). Review on potential use of fruit and vegetables by-products as a valuable source of natural food additives. *Food Science and Quality Management, 45*, 47–61.

Hanani, Z. A. N., Yee, F. C., & Nor-Khaizura, M. A. R. (2019). Effect of pomegranate (*Punica granatum L.*) peel powder on the antioxidant and antimicrobial properties of fish gelatin films as active packaging. *Food Hydrocolloids, 89*, 253–259. https://doi.org/10.1016/j.foodhyd.2018.10.007

Iyer, K. A., Zhang, L., & Torkelson, J. M. (2016). Direct use of natural antioxidant-rich agro-wastes as thermal stabilizer for polymer: Processing and recycling. *ACS Sustainable Chemistry & Engineering, 4*, 881–889. https://doi.org/10.1021/acssuschemeng.5b00945

Jamshidian, M., Tehrany, E. A., & Desobry, S. (2013). Antioxidants release from solvent-cast PLA film: Investigation of PLA antioxidant-active packaging. *Food and Bioprocess Technology, 6*(6), 1450–1463. https://doi.org/10.1007/s11947-012-0830-9

Jridi, M., Boughriba, S., Abdelhedi, O., Nciri, H., Nasri, R., Kchaou, H., Kaya, M., Sebai, H., Zouari, N., & Nasri, M. (2019). Investigation of physicochemical and antioxidant properties of gelatin edible film mixed with blood orange (*Citrus sinensis*) peel extract. *Food Packaging and Shelf Life, 21*, Article 100342. https://doi.org/10.1016/j.fpsl.2019.100342

Kang, H., Li, Y., Gong, M., Guo, Y., Guo, Z., Fang, Q., & Li, X. (2018). An environmentally sustainable plasticizer toughened polylactide. *RSC Advances, 8*, 11643.

Kannat, S., Jethwa, T., Sawant, K., & Chawla, S. (2017). PVA-gelatin films incorporated with tomato pulp: A potential primary food packaging film. *International Journal of Current Microbiology Applied Sciences, 6*, 1–14.

Khedkar, R., & Singh, K. (2018). Food industry waste: A panacea or pollution hazard? In T. Jindal (Ed.), *SpringerBriefs in environmental scienceParadigms in pollution prevention* (pp. 35–47). Cham: Springer International Publishing. https://doi.org/10.1007/978-3-319-58415-7_3.

August Kormin, S., Kormin, F., Beg, M. D. H., & Piah, M. B. M. (2017). Physical and mechanical properties of LDPE incorporated with different starch sources. In *IOP conference series: Materials science and engineering* (Vol. 226)IOP Publishing. https://doi.org/10.1088/1757-899X/226/1/012157. No. 1, p. 012157.

Kurek, M., Benbettaieb, N., Ščetar, M., Chaudy, E., Elez-Garofulić, I., Repajić, M., Klepac, D., Valić, S., Debaufort, F., & Galić, K. (2021). Novel functional chitosan and pectin bio-based packaging films with encapsulated Opuntia-ficus indica waste. *Food Bioscience, 41*, Article 100980. https://doi.org/10.1016/j.fbio.2021.100980

López-de-Dicastillo, C., Gómez-Estaca, J., Catalá, R., Gavara, R., & Hernández-Muñoz, P. (2012). Active antioxidant packaging films: Development and effect on lipid stability of brined sardines. *Food Chemistry, 131*(4), 1376–1384. https://doi.org/10.1016/j.foodchem.2011.10.002

Martí, R., Valcárcel, M., Herrero-Martínez, J. M., Cebolla-Cornejo, J., & Roselló, S. (2017). Simultaneous determination of main phenolic acids and flavonoids in tomato by micellar electrokinetic capillary electrophoresis. *Food Chemistry, 221*, 439–446. https://doi.org/10.1016/j.foodchem.2016.10.105

Menzel, C., González-Martínez, C., Vilaplana, F., Diretto, G., & Chiralt, A. (2020). Incorporation of natural antioxidants from rice straw into renewable starch films. *International Journal of Biological Macromolecules, 146*, 976–986. https://doi.org/10.1016/j.ijbiomac.2019.09.222

Pamuła, E., Błażewicz, M., Paluszkiewicz, C., & Dobrzyński, P. (2001). FTIR study of degradation products of aliphatic polyesters–carbon fibres composites. *Journal of Molecular Structure, 596*, 69–75. https://doi.org/10.1016/S0022-2860(01)00688-3

Park, S. I., & Zhao, Y. (2004). Incorporation of a high concentration of mineral or vitamin into chitosan-based films. *Journal of Agricultural and Food Chemistry, 52*(7), 1933–1939. https://doi.org/10.1021/jf034612p

Pereira de Abreu, D. A., Cruz, J. M., & Paseiro Losada, P. (2012). Active and intelligent packaging for the food industry. *Food Reviews International, 28*(2), 146–187. https://doi.org/10.1080/87559129.2011.595022

Peresin, M. S., Habibi, Y., Zoppe, J. O., Pawlak, J. J., & Rojas, O. J. (2010). Nanofiber composites of polyvinyl alcohol and cellulose nanocrystals: Manufacture and characterization. *Biomacromolecules, 11*(3), 674–681. https://doi.org/10.1021/bm901254n

Rangaraj, V. M., Devaraju, S., Rambabu, K., Banat, F., & Mittal, V. (2022). Silver-sepiolite (Ag-Sep) hybrid reinforced active gelatin/date waste extract (DSWE) blend composite films for food packaging application. *Food Chemistry, 369*, 130983. https://doi.org/10.1016/j.foodchem.2021.130983

Rangaraj, V. M., Rambabu, K., Banat, F., & Mittal, V. (2021). Effect of date fruit waste extract as an antioxidant additive on the properties of active gelatin films. *Food Chemistry, 355*, 129631. https://doi.org/10.1016/j.foodchem.2021.129631

Rhim, J. W., Gennadios, A., Weller, C. L., Cezeirat, C., & Hanna, M. A. (1998). Soy protein isolate-dialdehyde starch films. *Industrial Crops and Products, 8*(3), 195–203. https://doi.org/10.1016/S0926-6690(98)00003-X

Ribeiro, A. C. B., Cunha, A. P., Silva, L. M. R., Mattos, A. L. A., Brito, E. S., Filho, M. S. M. S., Azeredo, H. M. C., & Ricardo, N. M. P. S. (2021). From mango by-product to food packaging: Pectin-phenolic antioxidant films from mango peels. *International Journal of Biological Macromolecules, 193*, 1138–1150. https://doi.org/10.1016/j.ijbiomac.2021.10.131

December Russo, P., Speranza, V., Vignali, A., Tescione, F., Buonocore, G. G., & Lavorgna, M. (2015). Structure and physical properties of high amorphous polyvinyl alcohol/clay composites. In *AIP conference proceedings* (Vol. 1695)AIP Publishing LLC. https://doi.org/10.1063/1.4937313. No. 1, p. 020035.

Sanches-Silva, A., Costa, D., Albuquerque, T. G., Buonocore, G. G., Ramos, F., Castilho, M. C., Machado, A. V., & Costa, H. S. (2014). Trends in the use of natural antioxidants in active food packaging: A review. *Food Additives & Contaminants: Part A, 31*(3), 374–395. https://doi.org/10.1080/19440049.2013.879215

Stanzione, M., Gargiulo, N., Caputo, D., Liguori, B., Cerruti, P., Amendola, E., Lavorgna, M., & Buonocore, G. G. (2017). Peculiarities of vanillin release from amino-functionalized mesoporous silica embedded into biodegradable composites. *European Polymer Journal, 89C*, pp88–100.

Stanzione M, Zullo R, Buonocore GG, Lavorgna M. (2021) Effect of included bioactive compounds on barrier and mechanical properties of active packaging. Book chapter: Releasing systems in active food packaging: Preparation and applications - food

bioactive ingredients Volume: Vol. VIII, Pagine 550; Doi: 10.1007/978-3-030-90299-5; ISSN 2661-8958.

Stenmarck, Å., Jensen, C., Quested, T., Moates, G., Buksti, M., Cseh, B., & Östergren, K. (2016). *Estimates of European food waste levels*. IVL Swedish Environmental Research Institute.

Suñer, S., Joffe, R., Tipper, J. L., & Emami, N. (2015). Ultra high molecular weight polyethylene/graphene oxide nanocomposites: Thermal, mechanical and wettability characterisation. *Composites Part B: Engineering, 78*, 185–191.

Susmitha, A., Sasikumar, K., Rajan, D., Padmakumar, A. M., & Nampoothiri, K. M. (2021). Development and characterization of corn starch-gelatin based edible films incorporated with mango and pineapple for active packaging. *Food Bioscience, 41*, Article 100977. https://doi.org/10.1016/j.fbio.2021.100977

Tamasi, G., Pardini, A., Bonechi, C., Donati, A., Pessina, F., Marcolongo, P., … Rossi, C. (2019). Characterization of nutraceutical components in tomato pulp, skin and locular gel. *European Food Research and Technology, 245*(4), 907–918. https://doi.org/10.1007/s00217-019-03235-x

Valdés, A., Martínez, C., Garrigos, M. C., & Jiménez, A. (2021). Multilayer films based on poly(lactic acid)/gelatin supplemented with cellulose nanocrystals and antioxidant extract from almond shell by-product and its application on hass avocado preservation. *Polymers, 13*(21), 3615. https://doi.org/10.3390/polym13213615

Vallverdú-Queralt, A., Jáuregui, O., Lecce, G. D., Andrés-Lacueva, C., & Lamuela-Raventós, R. M. (2011). Screening of the polyphenol content of tomato-based products through accurate-mass spectrometry (HPLC–ESI-QTOF). *Food Chemistry, 129*, 877–883. https://doi.org/10.1016/j.foodchem.2011.05.03

Vilarinho, F., Stanzione, M., Buonocore, G. G., Barbosa-Pereira, L., Sendón, R., Vaz, M. F., & Silva, A. S. (2021). Green tea extract and nanocellulose embedded into polylactic acid film: Properties and efficiency on retarding the lipid oxidation of a model fatty food. *Food Packaging and Shelf Life, 27*, Article 100609. https://doi.org/10.1016/j.fpsl.2020.100609

Wang, L. F., & Rhim, J. W. (2016). Grapefruit seed extract incorporated antimicrobial LDPE and PLA films: Effect of type of polymer matrix. *Lebensmittel-Wissenschaft & Technologie, 74*, 338–345. https://doi.org/10.1016/j.lwt.2016.07.066

Wang, Y. L., Stanzione, M., Xia, H. S., Buonocore, G. G., Kaciulis, S., Fortunati, E., & Lavorgna, M. (2020). Effect of mercapto-silanes on the functional properties of highly amorphous vinyl alcohol composites with reduced graphene oxide and cellulose nanocrystals. *Composites Science and Technology, 200*, Article 108458. https://doi.org/10.1016/j.compscitech.2020.108458

Yoo, K. M., Lee, C. H., Lee, H., Moon, B., & Lee, C. Y. (2008). Relative antioxidant and cytoprotective activities of common herbs. *Food Chemistry, 106*(3), 929–936. https://doi.org/10.1016/j.foodchem.2007.07.006

Yusof, M. A., Nor Rahman, N. H., Sulaiman, S. Z., Sofian, A. H., Mat Desa, M. S. Z., & Izirwan, I. (2018). *Development of low density polyethylene/graphene nanoplatelets with enhanced thermal properties*. IEEE 9th International Conference on Mechanical and Intelligent Manufacturing Technologies.

Zeng, J., Ren, X., Zhu, S., & Gao, Y. (2021). Fabrication and characterization of an economical active packaging film based on chitosan incorporated with pomegranate peel. *International Journal of Biological Macromolecules, 192*, 1160–1168. https://doi.org/10.1016/j.ijbiomac.2021.10.064